Surface Science Spectra

RESEARCH ARTICLE | OCTOBER 10 2024

MgAlTi-LDH/gCN heterocomposites analyzed by x-ray photoelectron spectroscopy

Mattia Benedet ; Gian Andrea Rizzi ; Laura Marín ; Ivana Pavlovic ; Luis Sánchez ; Davide Barreca ; Chiara Maccato

Check for updates

Surf. Sci. Spectra 31, 024004 (2024)
https://doi.org/10.1116/6.0003896

View Online
Export Citation

Articles You May Be Interested In

KoopmanLab: Machine learning for solving complex physics equations

APL Mach. Learn. (September 2023)

Experimental realization of a quantum classification: Bell state measurement via machine learning

APL Mach. Learn. (September 2023)

10 October 2024 12:21:42

SSS SURFACE SCIENCE SPECTRA

ARTICLE

pubs.aip.org/avs/sss

MgAlTi-LDH/gCN heterocomposites analyzed by x-ray photoelectron spectroscopy

Cite as: Surf. Sci. Spectra **31**, 024004 (2024); doi: 10.1116/6.0003896
Submitted: 11 July 2024 · Accepted: 18 September 2024 ·
Published Online: 10 October 2024

View Online Export Citation CrossMark

Mattia Benedet,[1,2] Gian Andrea Rizzi,[1,2] Laura Marín,[3] Ivana Pavlovic,[3] Luis Sánchez,[3] Davide Barreca,[2,a)] and Chiara Maccato[1,2]

AFFILIATIONS

[1]Department of Chemical Sciences, Padova University and INSTM, 35131 Padova, Italy
[2]CNR-ICMATE and INSTM, Department of Chemical Sciences, Padova University, 35131 Padova, Italy
[3]Departamento de Química Inorgánica e Ingeniería Química, Instituto de Química para la Energía y el Medioambiente, Universidad de Córdoba, Campus de Rabanales, E-14014 Córdoba, Spain

Note: This paper is part of the 2024 Special Topic Collection on Materials for Energy and the Environment.
[a)]**Author to whom correspondence should be addressed:** davide.barreca@unipd.it

ABSTRACT

Layered double hydroxides (LDHs) and graphitic carbon nitride (gCN) are burgeoning multifunctional materials that have attracted a considerable interest as heterogeneous catalysts for environmental remediation. In the present work, we report on the x-ray photoelectron spectroscopy characterization of a representative MgAlTi-LDH/gCN heterocomposite, obtained by a simple mixing of single powdered constituents. Monochromated Al K_α radiation (1486.6 eV) was used as the source of x-ray excitation to acquire both wide-scan spectra and high-resolution signals of the principal element core levels. The main spectral features of the target system are critically examined and discussed in relation to the data related to the pristine MgAlTi-LDH. The obtained results highlight the occurrence of an electronic interplay between the single material constituents, anticipating an enhanced separation of photogenerated charge carriers and an improved activity for photocatalytic applications. The present reported data will serve as comparison for LDH-based materials obtained under various processing conditions for different end-uses.

10 October 2024 12:21:42

Key words: graphitic carbon nitride, layered double hydroxides, nanocomposites, x-ray photoelectron spectroscopy

© 2024 Author(s). All article content, except where otherwise noted, is licensed under a Creative Commons Attribution (CC BY) license (https://creativecommons.org/licenses/by/4.0/). https://doi.org/10.1116/6.0003896

Accession#: 01965 and 01966
Technique: X-ray photoelectron spectroscopy (XPS)
Specimen: MgAlTi-LDH; MgAlTi-LDH/gCN
Instrument: ThermoFisher Scientific EscalabTM QXi
Major Elements in Spectra: C, N, Mg, Al, Ti, and O
Minor Elements in Spectra: None
Published Spectra: 19
Spectral Category: Comparison

INTRODUCTION

The exponential growth of water and air pollution caused by the increasing industrialization represents a main threat for human health and for a sustainable development (Refs. 1–5). In this regard, over the last two decades, heterogeneous photocatalysis has emerged as an extremely promising avenue for the decomposition of aqueous and gaseous pollutants into nontoxic products, thanks to its efficiency, economic viability, and inherently green character (Refs. 1 and 5–8). Accordingly, considerable efforts worldwide have been dedicated by the scientific community to the design and fabrication of active photocatalysts effectively activated by solar energy, enabling the removal of pollutants from water and of nitrogen oxides from the outer atmosphere (Refs. 6 and 9–11). Among the possible alternatives, layered double hydroxides (LDHs) stand as very attractive functional platforms, thanks to the uniform metal dispersion, high structural flexibility, wide range of chemical

© Author(s) 2024

compositions, as well as tunable photoresponse range and surface chemistry (Refs. 1, 3, 4, 7, 9, and 12). Nonetheless, these advantages are at least partially eclipsed by the rapid recombination of photogenerated electrons and holes, limiting their efficiency (Refs. 1 and 2). In order to circumvent this drawback, a proficient option is offered by the combination of LDHs with other 2D materials, resulting in heterojunctions promoting the separation of electron-hole pairs and broadening the sunlight absorption spectrum (Refs. 1, 9, 13, and 14). To this aim, graphitic carbon nitride (gCN), a low-cost 2D semiconductor, is a very valuable candidate thanks to a plethora of favorable characteristics, encompassing non-toxicity, chemical stability, matching band structure, and excellent visible light response (Refs. 2, 4, 11, and 15–19).

In this general context, the present work is part of a comprehensive investigation aimed at the preparation and characterization of LDH-based heterogeneous photocatalysts for the removal of NO_x gases (x = 1 and 2) from urban environments (De-NO_x processes) (Refs. 3, 6, 9, 20, and 21). In particular, we focus on the study of LDH/gCN heterocomposites that, to our knowledge, have never been proposed for similar applications so far, at variance with bare gCN and LDHs (Refs. 7, 8, and 22). Since the system functional performances are directly affected by their structure, morphology, and chemical composition, we propose herein the investigation of MgAlTi-LDH/gCN systems prepared by a simple mixing procedure using x-ray photoelectron spectroscopy. Specifically, the attention is focused on the analysis of the main core levels (C 1*s*, Mg 1*s*, Mg 2*s*, Al 2*p*, Ti 2*p*, O 1*s*, and N 1*s*). The related spectral features reveal the formation of heterocomposites characterized by a direct electronic interplay between the system components, occurring through an interfacial gCN → MgAlTi-LDH charge transfer. These results, which anticipate an improved photocatalytic activity in comparison to the pristine LDH, may be of general interest for the scientific community working on the implementation of green photocatalysts for environmental remediation.

SPECIMEN DESCRIPTION (ACCESSION #01965)

Specimen: MgAlTi-LDH
CAS Registry #: Unknown
Specimen Characteristics: Homogeneous; powder; polycrystalline; semiconductor; inorganic compound; other
Chemical Name: Magnesium aluminum(III) titanium(IV) layered double hydroxide
Source: Specimen prepared by a coprecipitation method
Composition: C, Mg, Al, Ti, and O
Form: Supported nanocomposite
Structure: X-ray diffraction (XRD) analysis revealed the presence of signals located at 2θ = 11.2°, 22.5°, 34.5°, 38.7°; 45.8°, 60.2°, and 61.4°, attributable, respectively, to the (003), (006), (009), (015), (018), (110), and (113) crystallographic planes of $Mg_3Al_{0.8}Ti_{0.2}$ layered double hydroxide (Ref. 23).
History and Significance: $Mg_3Al_{0.8}Ti_{0.2}$ layered double hydroxide was prepared via coprecipitation. In particular, titanium(IV) tetraisopropoxide (TiO^iPr_4) was introduced dropwise for 45 min in a vessel containing concentrated HCl under a nitrogen atmosphere. The obtained $TiCl_4$ was subsequently introduced into a solution containing $MgCl_2$•$6H_2O$ and $AlCl_3$•$6H_2O$. The 100 ml resulting solution of metal salts with the suitable proportion [Mg(II)/(Al(III) + Ti(IV)) = 3 and Ti(IV)/Al(III) = 0.25] was gradually dropped into a Na_2CO_3•$10H_2O$ solution (100 ml) under stirring at room temperature, maintaining *p*H = 10 by the introduction of NaOH 4 M through an autotitrator. The resulting suspension was stirred for 16 h, washed with de-ionized water, and filtered. The obtained material was dried at 60 °C overnight. The delamination process was carried out following the AMOST (aqueous miscible organic solvent treatment) method (Refs. 3 and 24). In particular, the LDH was washed with de-ionized water until *p*H = 7 and subsequently with acetone (500 ml). The wet powders were then dispersed in 300 ml of acetone and stirred for 6 h at room temperature. The resulting product was then filtered, washed with 200 ml of acetone, and finally dried overnight at 60 °C.
As Received Condition: As grown
Analyzed Region: Same as the host material
***Ex Situ* Preparation/Mounting:** The powder was fixed to the sample holder using a copper double-sided adhesive tape.
***In Situ* Preparation:** Prior to analysis, the specimen was allowed to degas under vacuum conditions ($\times 10^{-7}$ mbar) at 298 K for 12 h.
Charge Control: Charge compensation was obtained by means of a dual-beam low energy electron and ion coaxial flood source (0.1 V, 175 μA, and gas cell at 20 V).
Temp. During Analysis: 298 K
Pressure During Analysis: 10^{-7} Pa
Pre-analysis Beam Exposure: 130 s

SPECIMEN DESCRIPTION (ACCESSION #01966)

Specimen: MgAlTi-LDH/gCN
CAS Registry #: Unknown
Specimen Characteristics: Homogeneous; powder; polycrystalline; semiconductor; composite; other
Chemical Name: Magnesium aluminum(III) titanium(IV) layered double hydroxide/graphitic carbon nitride
Source: Specimen prepared by mixing of single constituents
Composition: C, Mg, Al, Ti, and O
Form: Supported nanocomposite
Structure: XRD analysis yielded a diffraction pattern very similar to the one of bare MgAlTi-LDH (see accession #**01965**). The only difference was the presence of a weak signal at 2θ ≈ 28.2°, attributed to the (002) diffraction plane corresponding to the interplanar stacking of graphitic carbon nitride sheets (Refs. 15, 16, and 25).
History and Significance: The preparation of gCN powders was performed according to a previously reported synthetic route (Refs. 17 and 18). The target heterocomposite specimen was fabricated using a two-stage procedure. A mixture of $Mg_3Al_{0.8}Ti_{0.2}$ and gCN (285 and 15 mg, respectively) was suspended in 10 ml of deionized water. The slurry was stirred bar and heated to 40 °C. Subsequently, 10 ml of acetone was added to the mixture, and the stirring was continued at room temperature until complete solvent evaporation.
As Received Condition: As grown
Analyzed Region: Same as the host material

10 October 2024 12:21:42

© Author(s) 2024

***Ex Situ* Preparation/Mounting:** The powder was fixed to the sample holder using a copper double-sided adhesive tape.
***In Situ* Preparation:** Prior to analysis, the specimen was allowed to degas under vacuum conditions ($\approx 10^{-7}$ mbar) at 298 K for 12 h.
Charge Control: Charge compensation was obtained by means of a dual-beam low energy electron and ion coaxial flood source (0.1 V, 175 μA, and gas cell at 20 V).
Temp. During Analysis: 298 K
Pressure During Analysis: 10^{-7} Pa
Pre-analysis Beam Exposure: 130 s

INSTRUMENT DESCRIPTION

Manufacturer and Model: ThermoFisher Scientific EscalabTM QXi
Analyzer Type: Spherical sector
Detector: Channeltron
Number of Detector Elements: 6

INSTRUMENT PARAMETERS COMMON TO ALL SPECTRA

Spectrometer

Analyzer Mode: Constant pass energy
Throughput ($T = E^N$): Calculated from a cubic polynomial fit to a plot of log[peak area/(PE × RSF)] (y) versus log(KE/PE) (x): $y = a + bx + cx^2 + dx^3$, where PE is the pass energy, KE is the kinetic energy, and RSF is the relative sensitivity factor (Ref. 26). The coefficients corresponding to the adopted operating conditions are as follows: $a = 3.867\,64$; $b = -0.075\,012\,2$; $c = 0.003\,690\,77$; $d = -0.045\,752\,4$.
Excitation Source Window: None
Excitation Source: Al K_α monochromatic
Source Energy: 1486.6 eV
Source Strength: 200 W
Source Beam Size: $500 \times 500\ \mu m^2$
Signal Mode: Single channel direct

Geometry

Incident Angle: 58°
Source-to-Analyzer Angle: 58°
Emission Angle: 0°
Specimen Azimuthal Angle: 90°
Acceptance Angle from Analyzer Axis: 45°
Analyzer Angular Acceptance Width: 22.5° × 22.5°

Ion Gun

Manufacturer and Model: ThermoFisher Scientific MAGCIS Dual Beam Ion Source
Energy: 4000 eV
Current: 7 mA
Current Measurement Method: Biased stage
Sputtering Species and Charge: Ar^+
Spot Size (unrastered): 500 μm
Raster Size: $4500 \times 4500\ \mu m^2$
Incident Angle: 40°
Polar Angle: 40°
Azimuthal Angle: 270°
Comment: Differentially pumped ion gun

DATA ANALYSIS METHOD

Energy Scale Correction: The reported binding energies were corrected for charging phenomena by assigning a BE of 284.8 eV to the adventitious C 1*s* signal (Ref. 27).
Recommended Energy Scale Shift: +0.7 eV for accession #**01965** and +0.4 eV for accession #**01966**.
Peak Shape and Background Method: After performing a Shirley-type background subtraction (Ref. 28), least-squares fitting was performed adopting Gaussian/Lorentzian sum functions (% Lorentzian = 30%).
Quantitation Method: Atomic concentrations were calculated by peak area integration, using sensitivity factors provided by Thermo Scientific Avantage software (version 6.6.0, Build 00114).

ACKNOWLEDGMENTS

This work was financially supported by CNR (Progetti di Ricerca @CNR—avviso 2020-ASSIST), Padova University (Nos. P-DiSC#04BIRD2020-UNIPD EUREKA, P-DiSC#02BIRD2023-UNIPD RIGENERA, and DOR 2022-2024), INSTM21PDBARMAC-ATENA, PRIN No. 2022474YE8 (SCI-TROPHY project), finanziato dall'Unione Europea—Next Generation EU—Bando PRIN 2022—M4.C2.1.1, and Agencia Estatal de Investigación (Spain; No. MCIN PID2020-117516GB-l00/AEI/10.13039/501100011033). The used instrumentation was funded by "Sviluppo delle infrastrutture e programma biennale degli interventi del Consiglio Nazionale delle Ricerche (2019)."

10 October 2024 12:21:42

AUTHOR DECLARATIONS

Conflict of Interest

The authors have no conflicts to disclose.

Author Contributions

Mattia Benedet: Data curation (equal); Methodology (equal); Validation (equal); Visualization (equal); Writing – original draft (lead). **Gian Andrea Rizzi:** Data curation (equal); Funding acquisition (equal); Investigation (equal); Visualization (equal); Writing – review & editing (equal). **Laura Marín:** Investigation (equal); Software (equal); Validation (equal); Writing – review & editing (equal). **Ivana Pavlovic:** Data curation (equal); Investigation (equal); Validation (equal); Visualization (supporting). **Luis Sánchez:** Data curation (lead); Formal analysis (lead); Funding acquisition (equal); Investigation (equal); Methodology (equal); Writing – original draft (lead). **Davide Barreca:** Conceptualization (lead); Formal analysis (equal); Funding acquisition (equal); Supervision (equal); Writing – review & editing (lead). **Chiara Maccato:** Formal analysis (equal); Funding acquisition (equal); Methodology (equal); Supervision (lead); Visualization (lead); Writing – review & editing (equal).

© Author(s) 2024

DATA AVAILABILITY

The data that support the findings of this study are available within the article and its supplementary material.

REFERENCES

[1]Q. Chen *et al.*, J. Environ. Chem. Eng. **12**, 112806 (2024).
[2]M. Yang, P. Wang, Y. Li, S. Tang, X. Lin, H. Zhang, Z. Zhu, and F. Chen, Appl. Catal. B **306**, 121065 (2022).
[3]A. Pastor, C. Chen, G. de Miguel, F. Martin, M. Cruz-Yusta, J.-C. Buffet, D. O'Hare, I. Pavlovic, and L. Sánchez, Chem. Eng. J. **429**, 132361 (2022).
[4]X. Huang, X. Xu, R. Yang, and X. Fu, Colloids Surf. A **643**, 128738 (2022).
[5]G. Jiang, J. Cao, M. Chen, X. Zhang, and F. Dong, Appl. Surf. Sci. **458**, 77 (2018).
[6]J. Fragoso, A. Pastor, M. Cruz-Yusta, F. Martin, G. de Miguel, I. Pavlovic, M. Sánchez, and L. Sánchez, Appl. Catal. B **322**, 122115 (2023).
[7]X. Lv, J. Zhang, X. Dong, J. Pan, W. Zhang, W. Wang, G. Jiang, and F. Dong, Appl. Catal. B **277**, 119200 (2020).
[8]F. Dong, Z. Wang, Y. Li, W.-K. Ho, and S. C. Lee, Environ. Sci. Technol. **48**, 10345 (2014).
[9]A. Pastor, C. Chen, G. de Miguel, F. Martín, M. Cruz-Yusta, D. O'Hare, I. Pavlovic, and L. Sánchez, Chem. Eng. J. **471**, 144464 (2023).
[10]D. Barreca and C. Maccato, CrystEngComm **25**, 3968 (2023).
[11]Y. Yu, D. Chen, W. Xu, J. Fang, J. Sun, Z. Liu, Y. Chen, Y. Liang, and Z. Fang, J. Hazard. Mater. **416**, 126183 (2021).
[12]N. Chubar, V. Gerda, O. Megantari, M. Mičušík, M. Omastova, K. Heister, P. Man, and J. Fraissard, Chem. Eng. J. **234**, 284 (2013).
[13]A. Ali Khan and M. Tahir, ACS Appl. Energy Mater. **5**, 784 (2022).
[14]Y. Wu, H. Wang, Y. Sun, T. Xiao, W. Tu, X. Yuan, G. Zeng, S. Li, and J. W. Chew, Appl. Catal. B **227**, 530 (2018).
[15]M. Benedet, G. A. Rizzi, A. Gasparotto, N. Gauquelin, A. Orekhov, J. Verbeeck, C. Maccato, and D. Barreca, Appl. Surf. Sci. **618**, 156652 (2023).
[16]M. Benedet, G. A. Rizzi, A. Gasparotto, O. I. Lebedev, L. Girardi, C. Maccato, and D. Barreca, Chem. Eng. J. **448**, 137645 (2022).
[17]M. Benedet *et al.*, ACS Appl. Mater. Interfaces **15**, 47368 (2023).
[18]M. Benedet *et al.*, J. Mater. Chem. A **11**, 21595 (2023).
[19]Q. Xu, D. Ma, S. Yang, Z. Tian, B. Cheng, and J. Fan, Appl. Surf. Sci. **495**, 143555 (2019).
[20]J. Fragoso, M. A. Oliva, L. Camacho, M. Cruz-Yusta, G. de Miguel, F. Martin, A. Pastor, I. Pavlovic, and L. Sánchez, Chemosphere **275**, 130030 (2021).
[21]M. A. Oliva, D. Giraldo, P. Almodóvar, F. Martín, M. L. López, I. Pavlovic, and L. Sánchez, Chem. Eng. J. **489**, 151241 (2024).
[22]Z. Gu, Y. Asakura, and S. Yin, Nanotechnology **31**, 114001 (2020).
[23]JCPDS Card No. 41–1428.
[24]C. Chen, A. Wangriya, J.-C. Buffet, and D. O'Hare, Dalton Trans. **44**, 16392 (2015).
[25]F. Fina, S. K. Callear, G. M. Carins, and J. T. S. Irvine, Chem. Mater. **27**, 2612 (2015).
[26]M. Benedet, A. Gasparotto, G. A. Rizzi, C. Maccato, D. Mariotti, R. McGlynn, and D. Barreca, Surf. Sci. Spectra **30**, 024018 (2023).
[27]D. Briggs and M. P. Seah, *Practical Surface Analysis: Auger and X-ray Photoelectron Spectroscopy*, 2nd ed. (John Wiley & Sons, New York, 1990).
[28]D. A. Shirley, Phys. Rev. B **5**, 4709 (1972).
[29]J. F. Moulder, W. F. Stickle, P. E. Sobol, and K. D. Bomben, *Handbook of X-ray Photoelectron Spectroscopy* (Perkin Elmer Corporation, Eden Prairie, MN, 1992).
[30]M. Benedet, D. Barreca, G. A. Rizzi, C. Maccato, J.-L. Wree, A. Devi, and A. Gasparotto, Surf. Sci. Spectra **30**, 024021 (2023).
[31]M. Benedet, G. A. Rizzi, D. Barreca, A. Gasparotto, and C. Maccato, Surf. Sci. Spectra **30**, 014004 (2023).
[32]A. C. Reis Meira, J. V. G. Zago, B. Ghellere Tremarin, D. Z. Mezalira, A. C. Trindade Cursino, A. Bail, R. L. de Oliveira Basso, and R. M. Giona, J. Environ. Chem. Eng. **11**, 111443 (2023).
[33]Y. Bouvier, B. Mutel, and J. Grimblot, Surf. Coat. Technol. **180–181**, 169 (2004).
[34]J. I. Di Cosimo, V. K. Díez, M. Xu, E. Iglesia, and C. R. Apesteguía, J. Catal. **178**, 499 (1998).

10 October 2024 12:21:42

© Author(s) 2024

SPECTRAL FEATURES TABLE

Spectrum ID #	Element/ Transition	Peak Energy (eV)	Peak Width FWHM (eV)	Peak Area (eV × cts/s)	Sensitivity Factor	Concentration (at. %)	Peak Assignment
01965-02[a]	C 1*s*	284.8	2.0	17 797.8	1.000	2.3	Adventitious contamination
01965-02[a]	C 1*s*	288.5	2.0	47 395.6	1.000	6.0	Interlayer carbonate groups
01965-03	Mg 1*s*	1304.8	3.0	1611030.7	14.941	…	Mg(II) in MgAlTi-LDH
01965-04	Mg 2*s*	88.3	2.3	116503.2	0.757	18.2	Mg(II) in MgAlTi-LDH
01965-05	Mg 2*p*	49.6	1.7	57 198.3	0.429	…	Mg(II) in MgAlTi-LDH
01965-06	Mg $KL_{23}L_{23}$	306.2	—	—	—	—	Mg(II) in MgAlTi-LDH
01965-07	Al 2*p*	75.3	2.1	32 074.7	0.560	6.8	Al(III) in MgAlTi-LDH
01965-08[b]	Ti 2*p*	…	…	90 252.1	6.471	1.9	Ti(IV) in MgAlTi-LDH
01965-08	Ti $2p_{3/2}$	458.8	1.8	…	…	…	Ti(IV) in MgAlTi-LDH
01965-08	Ti $2p_{1/2}$	464.5	2.8	…	…	…	Ti(IV) in MgAlTi-LDH
01965-09[c]	O 1*s*	530.4	2.0	366146.7	2.881	17.8	M—O bonds
01965-09[c]	O 1*s*	531.5	2.0	697675.8	2.881	34.0	M—OH moieties and carbonate species
01965-09[c]	O 1*s*	533.0	2.0	267619.9	2.881	13.0	Adsorbed water
01966-02[a]	C 1*s*	284.8	1.9	9 444.3	1.000	1.2	Adventitious contamination
01966-02[a]	C 1*s*	286.4	2.1	20 682.9	1.000	2.7	C in C—NH_x (x = 1 and 2) groups
01966-02[a]	C 1*s*	288.5	2.2	64 315.3	1.000	8.2	N═C—N carbon atoms in gCN aromatic rings and interlayer carbonate groups
01966-03[d]	N 1*s*	398.9	2.0	16 834.0	1.676	1.3	Two-coordinated C═N—C nitrogen atoms from gCN
01966-03[d]	N 1*s*	400.1	1.8	9 397.2	1.676	0.8	Tertiary N—$(C)_3$ nitrogen atoms from gCN
01966-03[d]	N 1*s*	401.4	1.6	4 169.6	1.676	0.3	Uncondensed NH_x groups
01966-03[d]	N 1*s*	404.4	2.5	715.7	1.676	0.1	Excitation of π-electrons
01966-04	Mg 1*s*	1304.6	3.0	1492514.2	14.941	…	Mg(II) in MgAlTi-LDH
01966-05	Mg 2*s*	88.1	2.4	106966.4	0.757	17.0	Mg(II) in MgAlTi-LDH
01966-06	Mg 2*p*	49.4	1.8	57 067.0	0.429	…	Mg(II) in MgAlTi-LDH
01966-07	Mg $KL_{23}L_{23}$	306.0	—	—	—	—	Mg(II) in MgAlTi-LDH
01966-08	Al 2*p*	75.1	2.1	29 825.0	0.560	6.4	Al(III) in MgAlTi-LDH
01966-09[b]	Ti 2*p*			62 824.0	6.471	1.3	Ti(IV) in MgAlTi-LDH
01966-09	Ti $2p_{3/2}$	458.6	2.1	…	…	…	Ti(IV) in MgAlTi-LDH
01966-09	Ti $2p_{1/2}$	464.3	3.0	…	…	…	Ti(IV) in MgAlTi-LDH
01966-10[c]	O 1*s*	530.4	2.0	309398.4	2.881	15.3	M—O bonds
01966-10[c]	O 1*s*	531.5	2.1	793140.3	2.881	39.2	M—OH moieties and carbonate species

10 October 2024 12:21:42

© Author(s) 2024

(*Continued.*)

Spectrum ID #	Element/ Transition	Peak Energy (eV)	Peak Width FWHM (eV)	Peak Area (eV × cts/s)	Sensitivity Factor	Concentration (at. %)	Peak Assignment
01966-10[c]	O 1*s*	533.0	1.8	125232.7	2.881	6.2	Adsorbed water

[a]The sensitivity factor is referred to the whole C 1*s* signal.
[b]The peak area, sensitivity factor, and concentration are referred to the whole Ti 2*p* signal.
[c]The sensitivity factor is referred to the whole O 1*s* signal.
[d]The sensitivity factor is referred to the whole N 1*s* signal.

Footnote to Spectra 01965-01 and 01966-01: Wide-scan spectra were dominated by signals due to magnesium, aluminum, titanium, oxygen, and carbon. For accession **#01966** (see **01966-01**), the additional presence of nitrogen signals revealed the coexistence of MgAlTi-LDH and gCN.

Footnote to Spectra 01965-02 and 01966-02: For accession **#01965**, two different components contributed to the C 1 signal: the one related to adventitious contamination at BE = 284.8 eV (Refs. 17–19 and 27) and the one located at 288.5 eV, assigned to interlayer carbonate groups (Refs. 12 and 29) typically present in LDHs (Refs. 2, 3, 6, 9, 11, 13, and 20). In the case of accession **#01966**, the additional band centered at BE = 286.4 eV was ascribed to carbon in C—NH_x (x = 1 and 2) groups located on the heptazine ring edges in gCN (Refs. 15–17). The occurrence of these groups, which should not be present in the ideal (fully condensed) gCN structure, can result in an improved anchoring of gCN on MgAlTi-LDH (Ref. 30). For the same sample, the band positioned at 288.5 eV resulted from the concurrent contribution of the above-mentioned carbonate groups and of C in N—C═N groups belonging to gCN aromatic rings (Refs. 11, 18, and 22).

In comparison to bare gCN (Refs. 17 and 31), the BEs of the second and third components underwent an increase for accession **#01966** (+0.2 eV), in line with our recent studies on gCN-based composites (Refs. 26 and 30). Such a result suggested the formation of MgAlTi-LDH/gCN heterojunctions, responsible for gCN → MgAlTi-LDH electron transfer processes. A similar phenomenon, in turn, promoted an improved separation of photoproduced electrons and holes, paving the way to a higher photocatalytic activity for the composite system, of relevance in view of eventual applications. These conclusions were further supported by the analysis of nitrogen and metal photopeaks (compare the following comments).

Footnote to Spectra 01965-03, 01965-05, 01965-06, 01965-07, 01965-08, 01966-04, 01966-06, 01966-07, 01965-08, and 01966-09: The energy positions of the principal magnesium, aluminum, and titanium core level peaks (Mg 1*s*, Al 2*p*, and Ti 2*p*, respectively) were compatible with those reported for Mg(II) (Refs. 7, 11, and 12), Al(III) (Refs. 1, 4, and 12), and Ti(IV) (Refs. 5 and 6), free from other oxidation states in appreciable amounts. The Mg $KL_{23}L_{23}$ BE was in line with the one recently reported for magnesium-aluminum layered double hydroxides (Ref. 32).

Calculation of magnesium Auger parameter [α = BE(Mg 2*p*) + KE (Mg $KL_{23}L_{23}$)] yielded 1230.0 eV for both the target accessions, a value relatively close to those previously reported for various oxygenated Mg compounds (Ref. 27). Taking into account that the Mg 1*s* peak shows a higher photoemission cross section than the Mg 2p one, an alternative definition of the Mg Auger parameter has also been proposed (Ref. 33): α^* = KE(Mg $KL_{23}L_{23}$) – KE (Mg 1*s*). The obtained α^* values were both 998.6 eV, in the range reported for magnesium hydroxides/carbonates (Ref. 33).

As can be observed, the BEs of the metal photoelectron peaks were red-shifted (−0.2 eV) upon passing from MgAlTi-LDH to MgAlTi-LDH/gCN. This variation, of the same magnitude, but opposite sign with respect to that exhibited by the aforementioned C 1*s* components, corroborated the direct integration of MgAlTi-LDH and gCN in the target composite, with the gCN → MgAlTi-LDH electron transfer due to type-II heterojunction formation.

An inspection of the Spectral Features Table reveals that the surface Mg/Al ratio for both the analyzed specimens is very close to 2.70, i.e., lower than the bulk ratio, corresponding to 3.75 as calculated for $Mg_3Al_{0.8}Ti_{0.2}$ (see the above-reported structural data for both specimens). This result may suggest an Al surface segregation, in accordance with previously reported results (Ref. 34). The opposite trend is observed for Ti, basing on the comparison of the surface Mg/Ti ratio with the value of 3.75 deduced from the above-reported formula.

Footnote to Spectrum 01965-04 and 01966-05: As already performed by other investigators (Ref. 34), the Mg 2*s* photopeak was recorded to obtain a more accurate evaluation of atomic percentages. In fact, the use of the most intense magnesium signal, Mg 1*s*, is not the best choice to this purpose due to the appreciable BE difference with the other peaks. This feature would imply the analysis of photoelectrons with different escape depths, yielding, thus, alterations in the obtained values (Ref. 27).

Footnote to Spectrum 01966-03: As typically observed for graphitic carbon nitride systems (Refs. 15 and 18), the N 1*s* signal resulted from four distinct components. The most intense one (BE = 398.9 eV) was due to nitrogen in C═N—C groups (Refs. 1, 15, and 18), whereas the band at 400.1 eV was attributed to tri-coordinated N atoms belonging to N—$(C)_3$ moieties (Refs. 2, 8, and 18). In accordance with the outcomes of C 1*s* analysis (see above), the component located at 401.4 eV was attributed to N in uncondensed amino groups C—NH_x (Refs. 1, 17, and 18). Finally, the weaker high BE band at 404.4 eV was due to π-electron excitations in heptazine rings (Refs. 11 and 15).

In agreement with the data pertaining to the C 1*s* signal (see Footnote to Spectra **01965-02** and **01966-02**), all the N1*s* components underwent a positive energy shift corresponding to +0.2 eV with respect to pure gCN (Refs. 17 and 31), confirming the above-reported electronic interplay related to the occurrence of MgAlTi-LDH/gCN heterojunctions.

Footnote to Spectrum 01965-09 and 01966-10: The O 1*s* signals were characterized by the concurrent contribution of three peaks corresponding to M—O bonds (O_1) (Refs. 9 and 14), M—OH and carbonate species (Refs. 7, 20, and 21), and adsorbed water (Refs. 21 and 29).

10 October 2024 12:21:42

© Author(s) 2024

ANALYZER CALIBRATION TABLE

Spectrum ID #	Element/ Transition	Peak Energy (eV)	Peak Width FWHM (eV)	Peak Area (eV × cts/s)	Sensitivity Factor	Concentration (at. %)	Peak Assignment
…	Au $4f_{7/2}$	84.0	1.1	2 841 305.7	20.735	…	Au(0)
…	Cu $2p_{3/2}$	932.7	1.3	5 350 621.8	26.513	…	Cu(0)

Comment to Analyzer Calibration Table: The peaks were acquired after Ar^+ erosion.

GUIDE TO FIGURES

Spectrum (Accession) #	Spectral Region	Voltage Shift[a]	Multiplier	Baseline	Comment #
01965-01	Survey	–0.7	1	0	…
01965-02	C 1*s*	–0.7	1	0	…
01965-03	Mg 1*s*	–0.7	1	0	…
01965-04	Mg 2*s*	–0.7	1	0	…
01965-05	Mg 2*p*	0.7	1	0	…
01965-06	Mg $KL_{23}L_{23}$	+0.7	1	0	…
01965-07	Al 2*p*	–0.7	1	0	…
01965-08	Ti 2*p*	–0.7	1	0	…
01965-09	O 1*s*	–0.7	1	0	…
01966-01	Survey	–0.4	1	0	…
01966-02	C 1*s*	–0.4	1	0	…
01966-03	N 1*s*	–0.4	1	0	…
01966-04	Mg 1*s*	–0.4	1	0	…
01966-05	Mg 2*s*	–0.4	1	0	…
01966-06	Mg 2*p*	–0.4	1	0	…
01966-07	Mg $KL_{23}L_{23}$	+0.4	1	0	…
01966-08	Al 2*p*	–0.4	1	0	…
01966-09	Ti 2*p*	–0.4	1	0	…
01966-10	O 1*s*	–0.4	1	0	…

[a]Voltage shift of the archived (as-measured) spectrum relative to the printed figure. The figure reflects the recommended energy scale correction due to a calibration correction, sample charging, flood gun, or other phenomenon.

10 October 2024 12:21:42

© Author(s) 2024

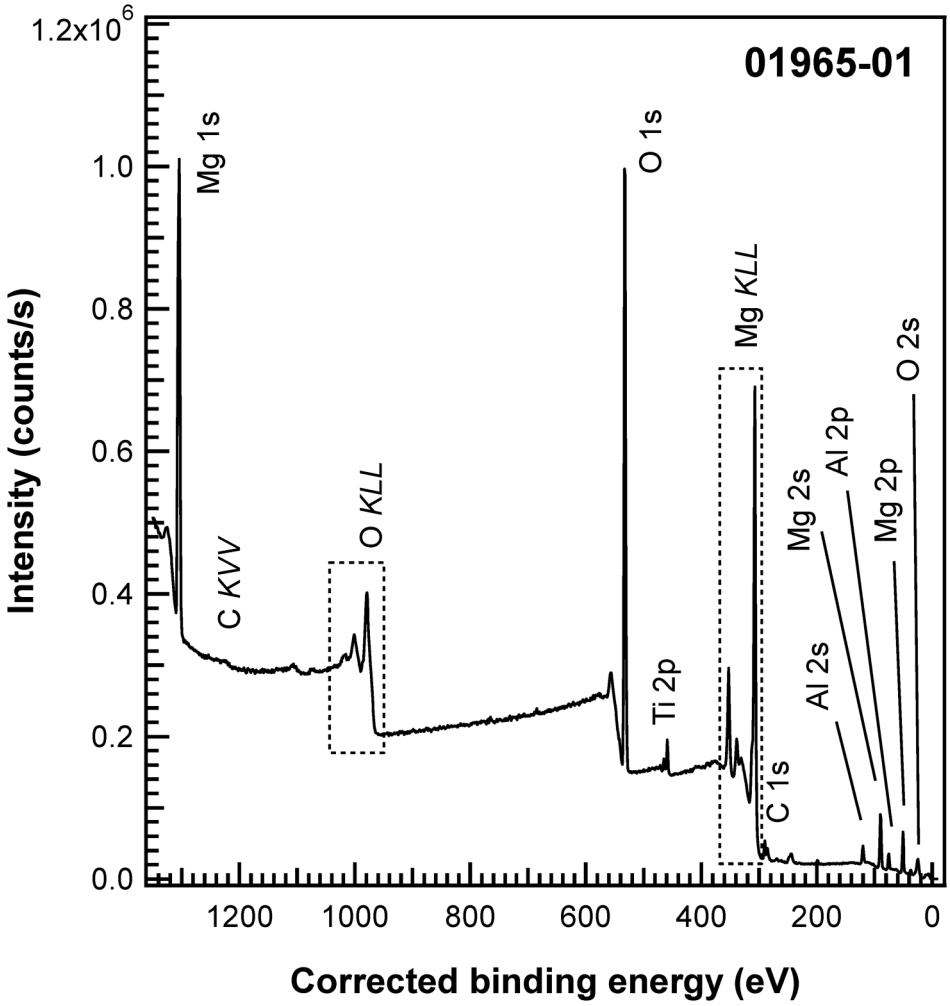

10 October 2024 12:21:42

Accession #:	01965-01
■ Specimen:	MgAlTi-LDH
■ Technique:	XPS
■ Spectral Region:	Survey
Instrument:	ThermoFisher Scientific EscalabTM QXi
Excitation Source:	Al K_α monochromatic
Source Energy:	1486.6 eV
Source Strength:	200 W
Source Size:	0.50 × 0.50 mm^2
Analyzer Type:	Spherical sector
Incident Angle:	58°
Emission Angle:	0°
Analyzer Pass Energy:	80 eV
Analyzer Resolution:	0.8 eV
Total Signal Accumulation Time:	136.1 s
Total Elapsed Time:	149.7 s
Number of Scans:	2
Effective Detector Width:	0.8 eV

© Author(s) 2024

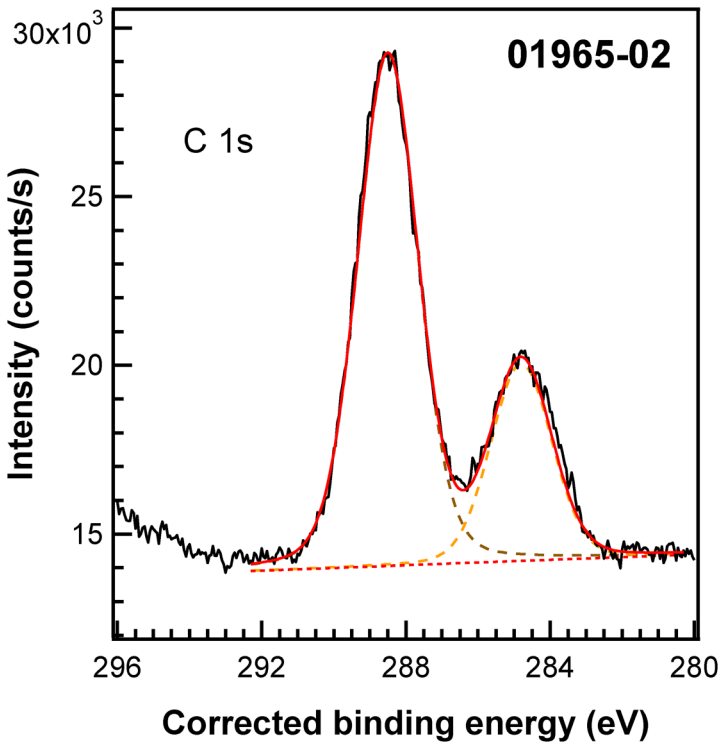

- **Accession #:** 01965-02
- **Specimen:** MgAlTi-LDH
- **Technique:** XPS
- **Spectral Region:** C 1*s*

Instrument: ThermoFisher Scientific EscalabTM QXi
Excitation Source: Al K_α monochromatic
Source Energy: 1486.6 eV
Source Strength: 200 W
Source Size: 0.50 × 0.50 mm^2
Analyzer Type: Spherical sector
Incident Angle: 58°
Emission Angle: 0°
Analyzer Pass Energy: 50 eV
Analyzer Resolution: 0.5 eV
Total Signal Accumulation Time: 114.3 s
Total Elapsed Time: 125.7 s
Number of Scans: 3
Effective Detector Width: 0.5 eV

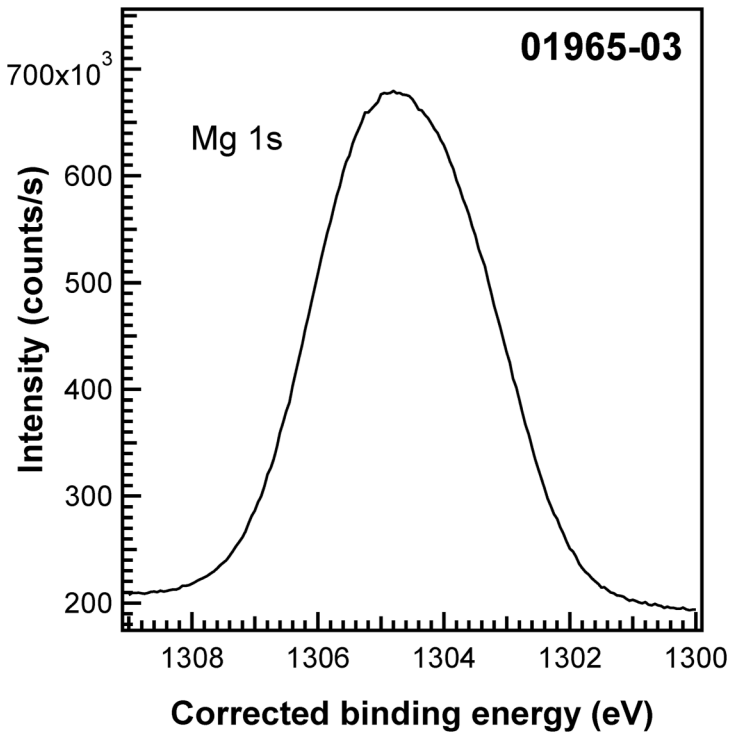

- **Accession #:** 01965-03
- **Specimen:** MgAlTi-LDH
- **Technique:** XPS
- **Spectral Region:** Mg 1*s*

Instrument: ThermoFisher Scientific EscalabTM QXi
Excitation Source: Al K_α monochromatic
Source Energy: 1486.6 eV
Source Strength: 200 W
Source Size: 0.50 × 0.50 mm^2
Analyzer Type: Spherical sector
Incident Angle: 58°
Emission Angle: 0°
Analyzer Pass Energy: 50 eV
Analyzer Resolution: 0.5 eV
Total Signal Accumulation Time: 60.2 s
Total Elapsed Time: 66.2 s
Number of Scans: 2
Effective Detector Width: 0.5 eV

10 October 2024 12:21:42

© Author(s) 2024

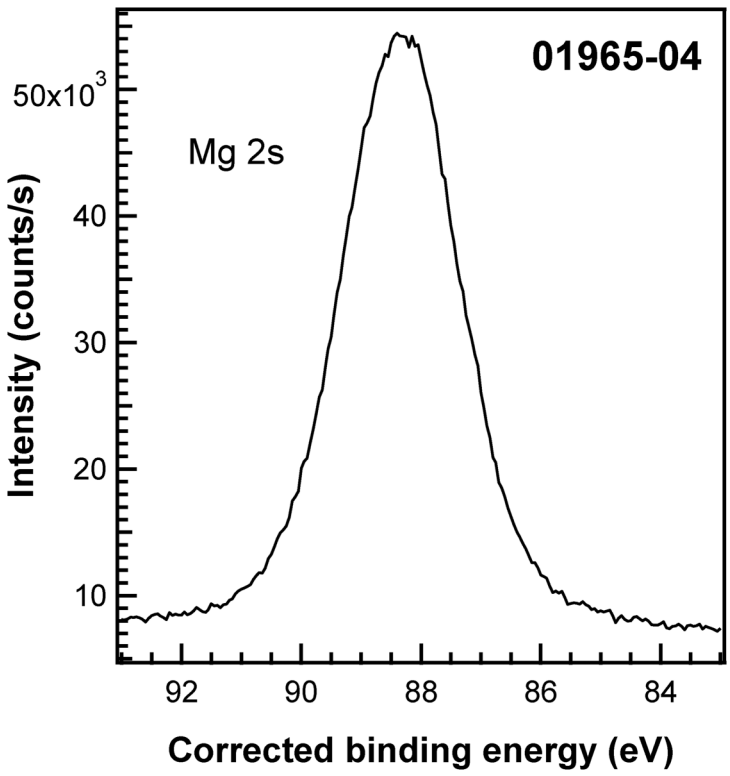

- **Accession #:** 01965-04
- **Specimen:** MgAlTi-LDH
- **Technique:** XPS
- **Spectral Region:** Mg 2*s*

Instrument: ThermoFisher Scientific EscalabTM QXi
Excitation Source: Al K_α monochromatic
Source Energy: 1486.6 eV
Source Strength: 200 W
Source Size: 0.50 × 0.50 mm^2
Analyzer Type: Spherical sector
Incident Angle: 58°
Emission Angle: 0°
Analyzer Pass Energy: 50 eV
Analyzer Resolution: 0.5 eV
Total Signal Accumulation Time: 48.2 s
Total Elapsed Time: 53.0 s
Number of Scans: 2
Effective Detector Width: 0.5 eV

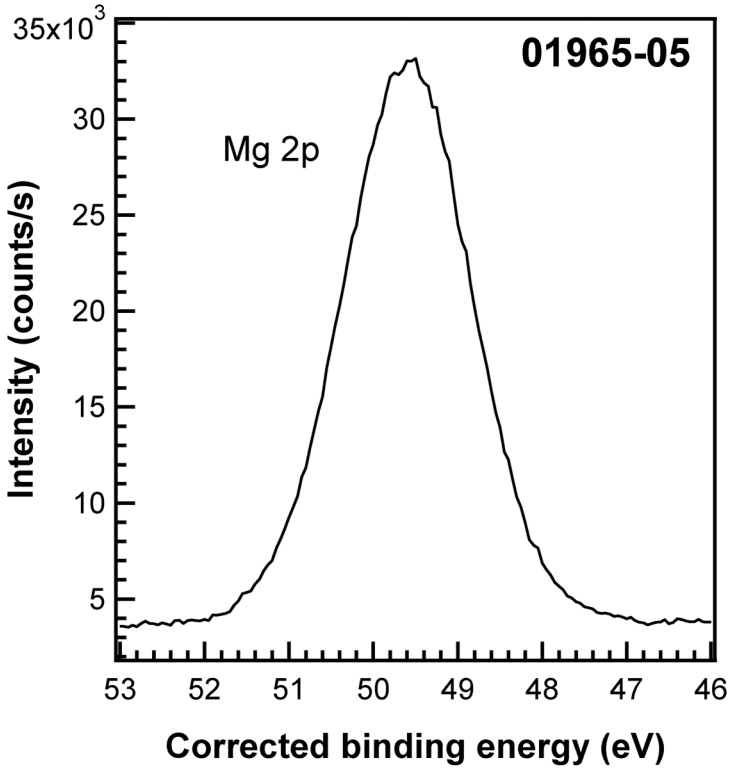

- **Accession #:** 01965-05
- **Specimen:** MgAlTi-LDH
- **Technique:** XPS
- **Spectral Region:** Mg 2p

Instrument: ThermoFisher Scientific EscalabTM QXi
Excitation Source: Al K_α monochromatic
Source Energy: 1486.6 eV
Source Strength: 200 W
Source Size: 0.50 × 0.50 mm^2
Analyzer Type: Spherical sector
Incident Angle: 58°
Emission Angle: 0°
Analyzer Pass Energy: 50 eV
Analyzer Resolution: 0.5 eV
Total Signal Accumulation Time: 108.3 s
Total Elapsed Time: 119.1 s
Number of Scans: 3
Effective Detector Width: 0.5 eV

10 October 2024 12:21:42

© Author(s) 2024

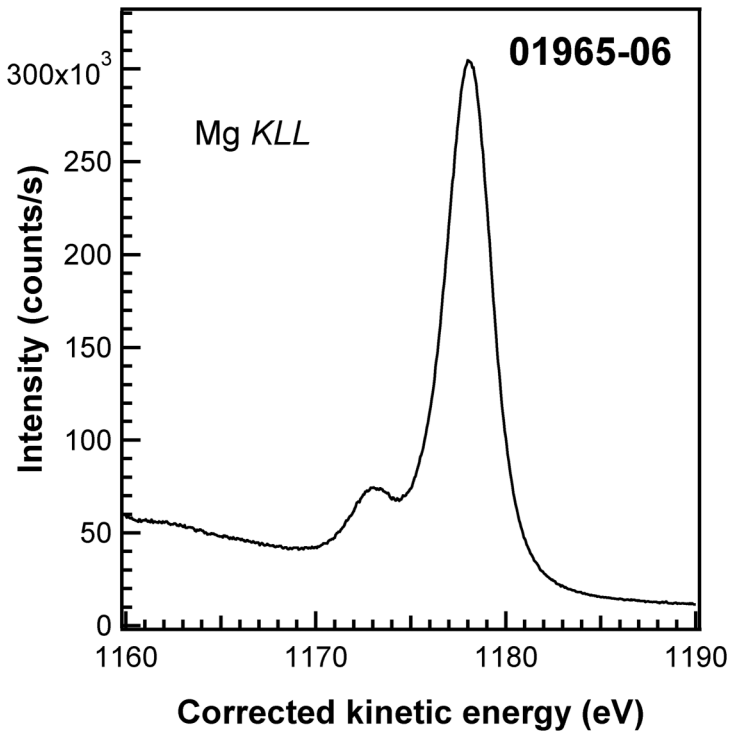

- **Accession #:** 01965-06
- **Specimen:** MgAlTi-LDH
- **Technique:** XPS
- **Spectral Region:** Mg KLL

Instrument: ThermoFisher Scientific EscalabTM QXi
Excitation Source: Al K_α monochromatic
Source Energy: 1486.6 eV
Source Strength: 200 W
Source Size: 0.50 × 0.50 mm^2
Analyzer Type: Spherical sector
Incident Angle: 58°
Emission Angle: 0°
Analyzer Pass Energy: 50 eV
Analyzer Resolution: 0.5 eV
Total Signal Accumulation Time: 152.2 s
Total Elapsed Time: 167.4 s
Number of Scans: 2
Effective Detector Width: 0.5 eV

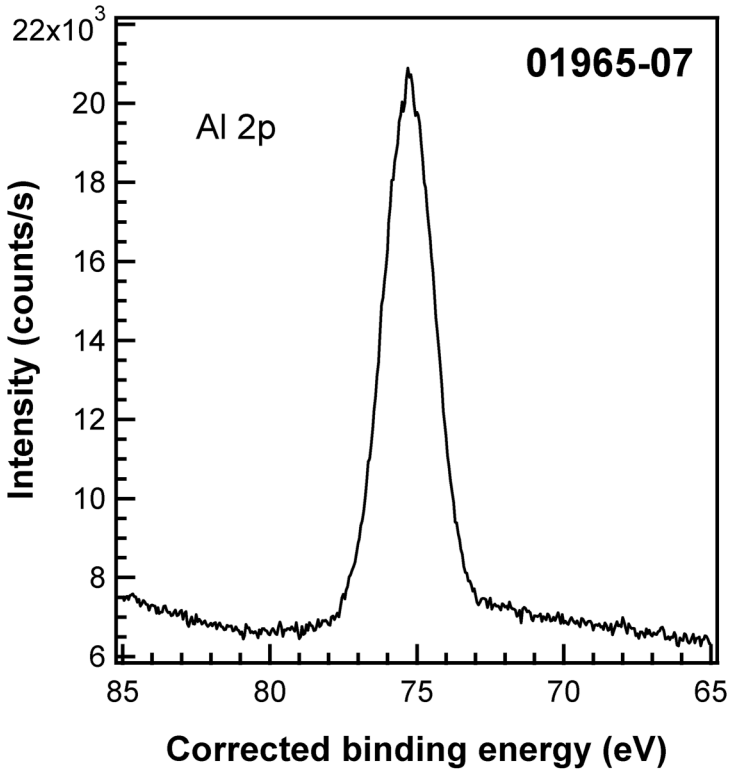

- **Accession #:** 01965-07
- **Specimen:** MgAlTi-LDH
- **Technique:** XPS
- **Spectral Region:** Al 2*p*

Instrument: ThermoFisher Scientific EscalabTM QXi
Excitation Source: Al K_α monochromatic
Source Energy: 1486.6 eV
Source Strength: 200 W
Source Size: 0.50 × 0.50 mm^2
Analyzer Type: Spherical sector
Incident Angle: 58°
Emission Angle: 0°
Analyzer Pass Energy: 50 eV
Analyzer Resolution: 0.5 eV
Total Signal Accumulation Time: 200.5 s
Total Elapsed Time: 220.6 s
Number of Scans: 5
Effective Detector Width: 0.5 eV

10 October 2024 12:21:42

© Author(s) 2024

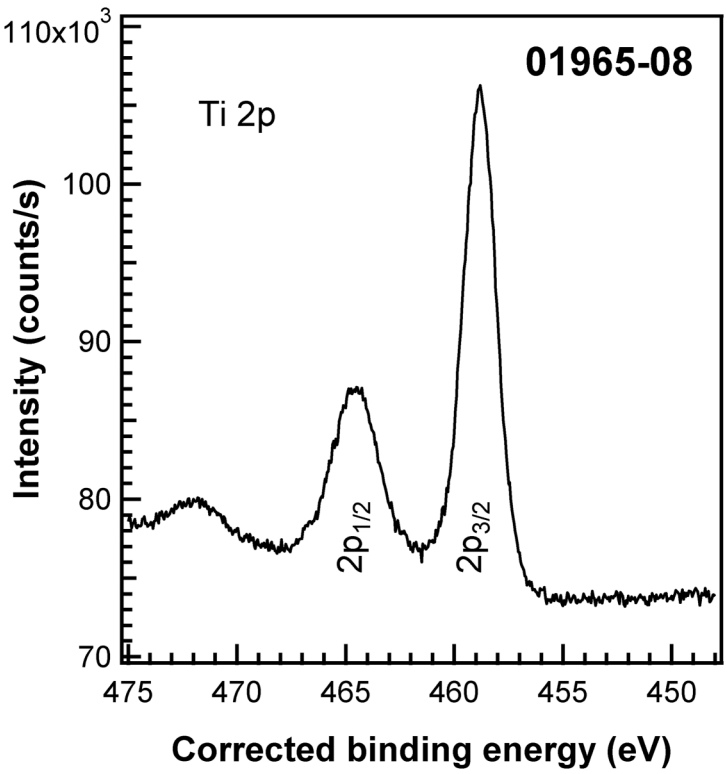

- **Accession #:** 01965-08
- **Specimen:** MgAlTi-LDH
- **Technique:** XPS
- **Spectral Region:** Ti 2*p*

Instrument: ThermoFisher Scientific EscalabTM QXi
Excitation Source: Al K_α monochromatic
Source Energy: 1486.6 eV
Source Strength: 200 W
Source Size: 0.50 × 0.50 mm^2
Analyzer Type: Spherical sector
Incident Angle: 58°
Emission Angle: 0°
Analyzer Pass Energy: 50 eV
Analyzer Resolution: 0.5 eV
Total Signal Accumulation Time: 432.8 s
Total Elapsed Time: 476.1 s
Number of Scans: 8
Effective Detector Width: 0.5 eV

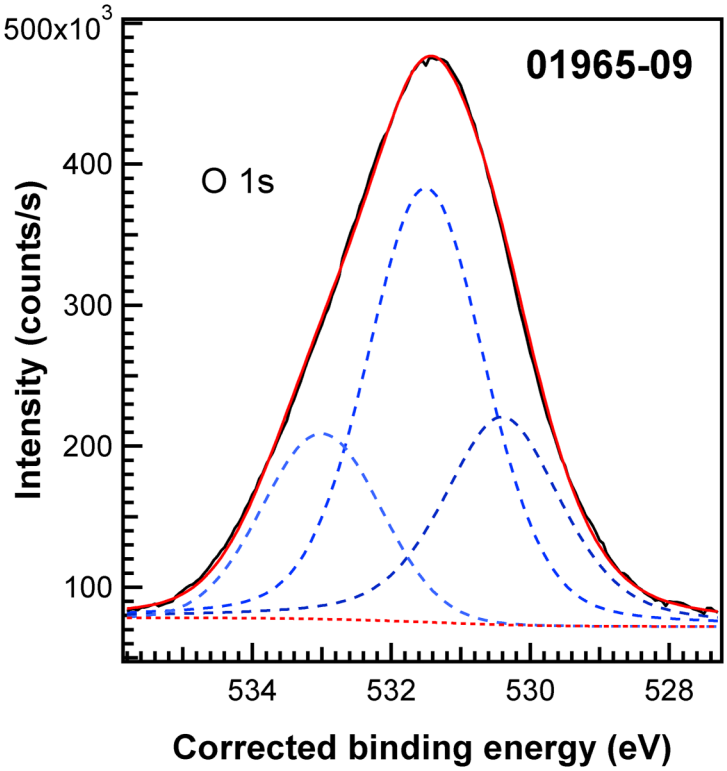

- **Accession #:** 01965-09
- **Specimen:** MgAlTi-LDH
- **Technique:** XPS
- **Spectral Region:** O 1*s*

Instrument: ThermoFisher Scientific EscalabTM QXi
Excitation Source: Al K_α monochromatic
Source Energy: 1486.6 eV
Source Strength: 200 W
Source Size: 0.50 × 0.50 mm^2
Analyzer Type: Spherical sector
Incident Angle: 58°
Emission Angle: 0°
Analyzer Pass Energy: 50 eV
Analyzer Resolution: 0.5 eV
Total Signal Accumulation Time: 80.2 s
Total Elapsed Time: 88.2 s
Number of Scans: 2
Effective Detector Width: 0.5 eV

10 October 2024 12:21:42

© Author(s) 2024

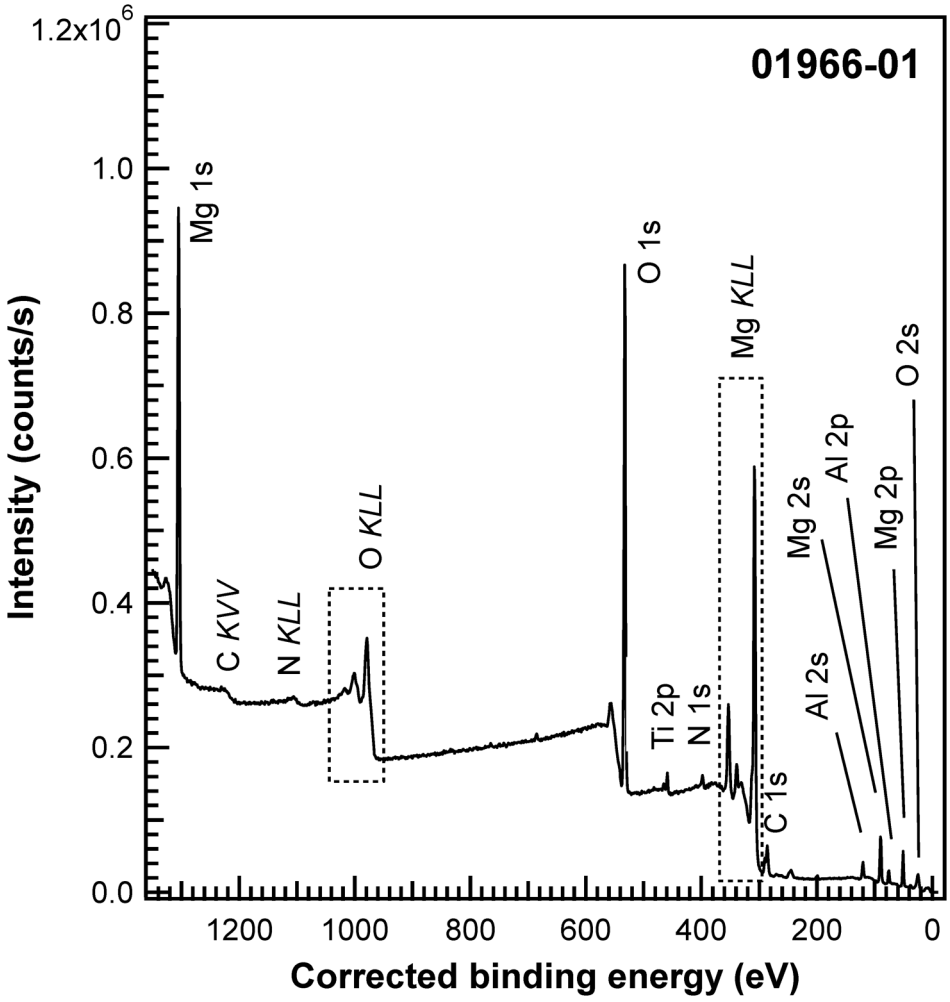

10 October 2024 12:21:42

Accession #:	01966-01
■ Specimen:	MgAlTi-LDH/gCN
■ Technique:	XPS
■ Spectral Region:	Survey
Instrument:	ThermoFisher Scientific EscalabTM QXi
Excitation Source:	Al K_α monochromatic
Source Energy:	1486.6 eV
Source Strength:	200 W
Source Size:	0.50 × 0.50 mm^2
Analyzer Type:	Spherical sector
Incident Angle:	58°
Emission Angle:	0°
Analyzer Pass Energy:	80 eV
Analyzer Resolution:	0.8 eV
Total Signal Accumulation Time:	136.1 s
Total Elapsed Time:	149.7 s
Number of Scans:	2
Effective Detector Width:	0.8 eV

© Author(s) 2024

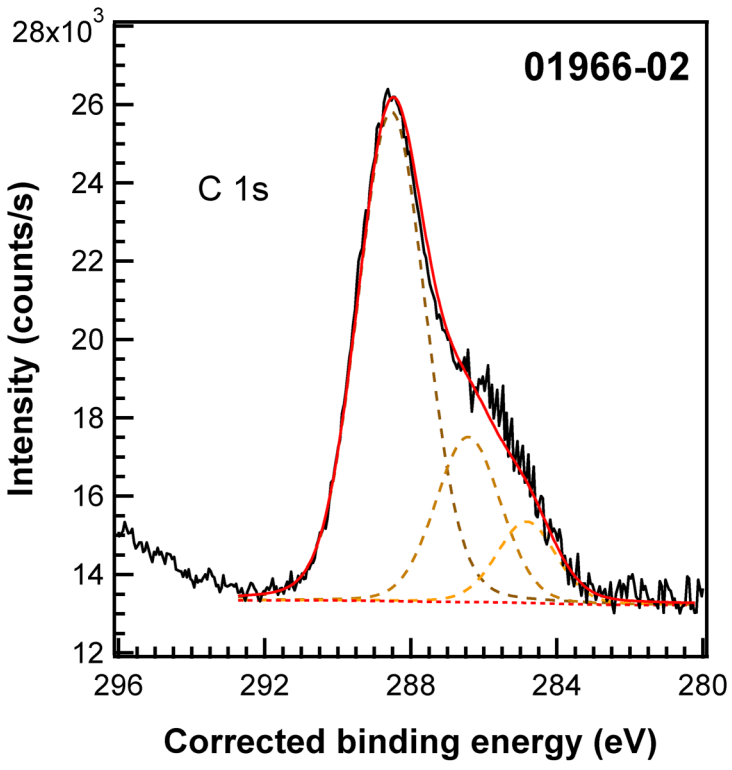

- **Accession #:** 01966-02
- **Specimen:** MgAlTi-LDH/gCN
- **Technique:** XPS
- **Spectral Region:** C 1*s*

Instrument: ThermoFisher Scientific EscalabTM QXi
Excitation Source: Al K_α monochromatic
Source Energy: 1486.6 eV
Source Strength: 200 W
Source Size: 0.50 × 0.50 mm^2
Analyzer Type: Spherical sector
Incident Angle: 58°
Emission Angle: 0°
Analyzer Pass Energy: 50 eV
Analyzer Resolution: 0.5 eV
Total Signal Accumulation Time: 190.5 s
Total Elapsed Time: 209.6 s
Number of Scans: 5
Effective Detector Width: 0.5 eV

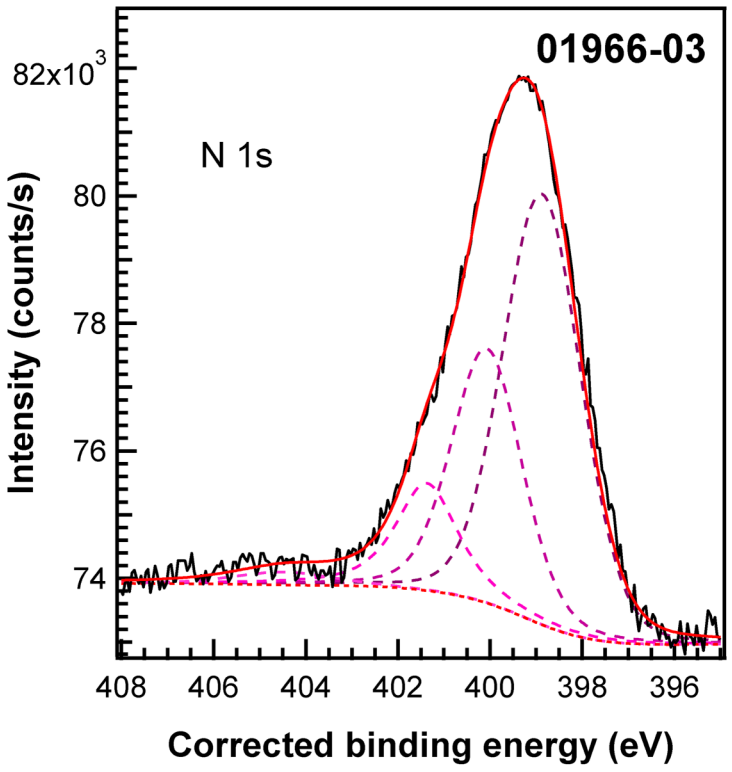

- **Accession #:** 01966-03
- **Specimen:** MgAlTi-LDH/gCN
- **Technique:** XPS
- **Spectral Region:** N 1*s*

Instrument: ThermoFisher Scientific EscalabTM QXi
Excitation Source: Al K_α monochromatic
Source Energy: 1486.6 eV
Source Strength: 200 W
Source Size: 0.50 × 0.50 mm^2
Analyzer Type: Spherical sector
Incident Angle: 58°
Emission Angle: 0°
Analyzer Pass Energy: 50 eV
Analyzer Resolution: 0.5 eV
Total Signal Accumulation Time: 802.0 s
Total Elapsed Time: 882.2 s
Number of Scans: 20
Effective Detector Width: 0.5 eV

10 October 2024 12:21:42

© Author(s) 2024

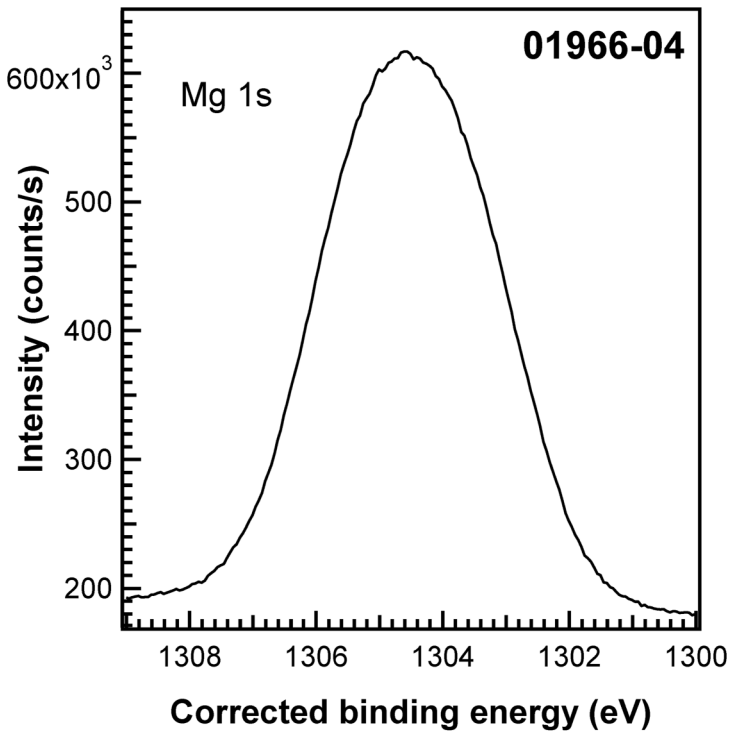

- **Accession #:** 01966-04
- **Specimen:** MgAlTi-LDH/gCN
- **Technique:** XPS
- **Spectral Region:** Mg 1*s*

Instrument: ThermoFisher Scientific EscalabTM QXi
Excitation Source: Al K_α monochromatic
Source Energy: 1486.6 eV
Source Strength: 200 W
Source Size: 0.50 × 0.50 mm^2
Analyzer Type: Spherical sector
Incident Angle: 58°
Emission Angle: 0°
Analyzer Pass Energy: 50 eV
Analyzer Resolution: 0.5 eV
Total Signal Accumulation Time: 60.2 s
Total Elapsed Time: 66.2 s
Number of Scans: 2
Effective Detector Width: 0.5 eV

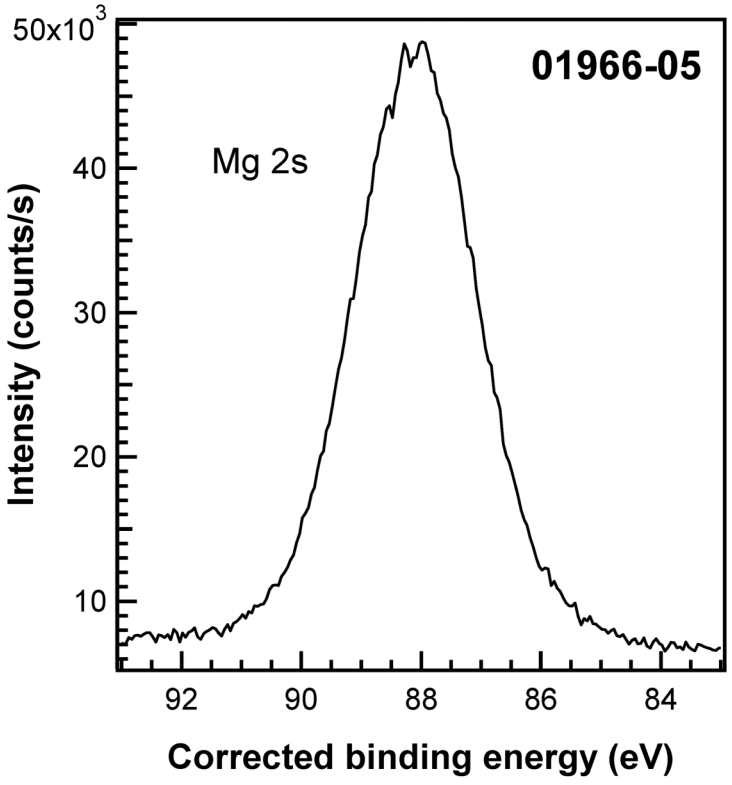

- **Accession #:** 01966-05
- **Specimen:** MgAlTi-LDH/gCN
- **Technique:** XPS
- **Spectral Region:** Mg 2*s*

Instrument: ThermoFisher Scientific EscalabTM QXi
Excitation Source: Al K_α monochromatic
Source Energy: 1486.6 eV
Source Strength: 200 W
Source Size: 0.50 × 0.50 mm^2
Analyzer Type: Spherical sector
Incident Angle: 58°
Emission Angle: 0°
Analyzer Pass Energy: 50 eV
Analyzer Resolution: 0.5 eV
Total Signal Accumulation Time: 48.2 s
Total Elapsed Time: 53.0 s
Number of Scans: 2
Effective Detector Width: 0.5 eV

10 October 2024 12:21:42

© Author(s) 2024

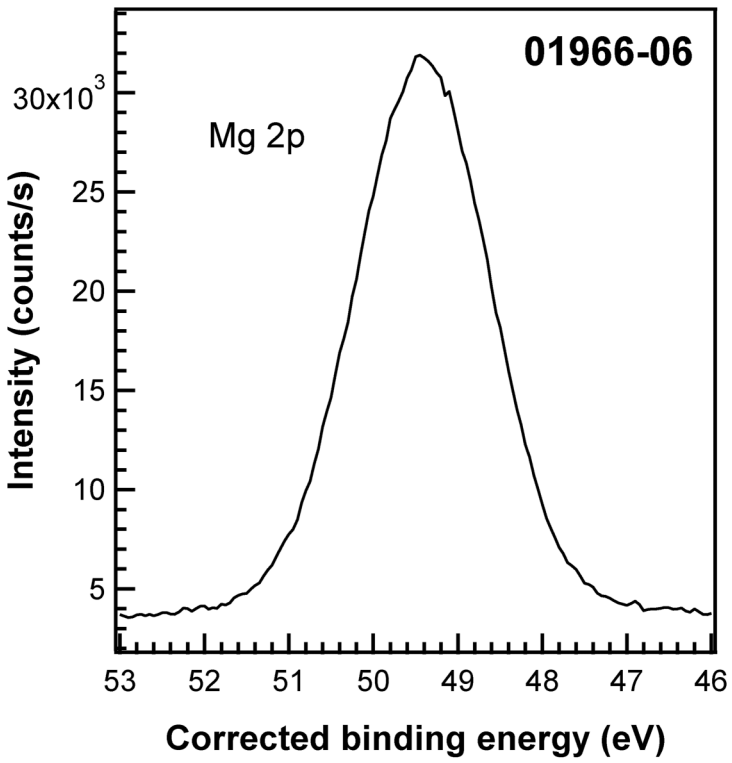

- **Accession #:** 01965-06
- **Specimen:** MgAlTi-LDH/gCN
- **Technique:** XPS
- **Spectral Region:** Mg 2p

Instrument: ThermoFisher Scientific EscalabTM QXi
Excitation Source: Al K_α monochromatic
Source Energy: 1486.6 eV
Source Strength: 200 W
Source Size: 0.50 × 0.50 mm^2
Analyzer Type: Spherical sector
Incident Angle: 58°
Emission Angle: 0°
Analyzer Pass Energy: 50 eV
Analyzer Resolution: 0.5 eV
Total Signal Accumulation Time: 108.3 s
Total Elapsed Time: 119.1 s
Number of Scans: 3
Effective Detector Width: 0.5 eV

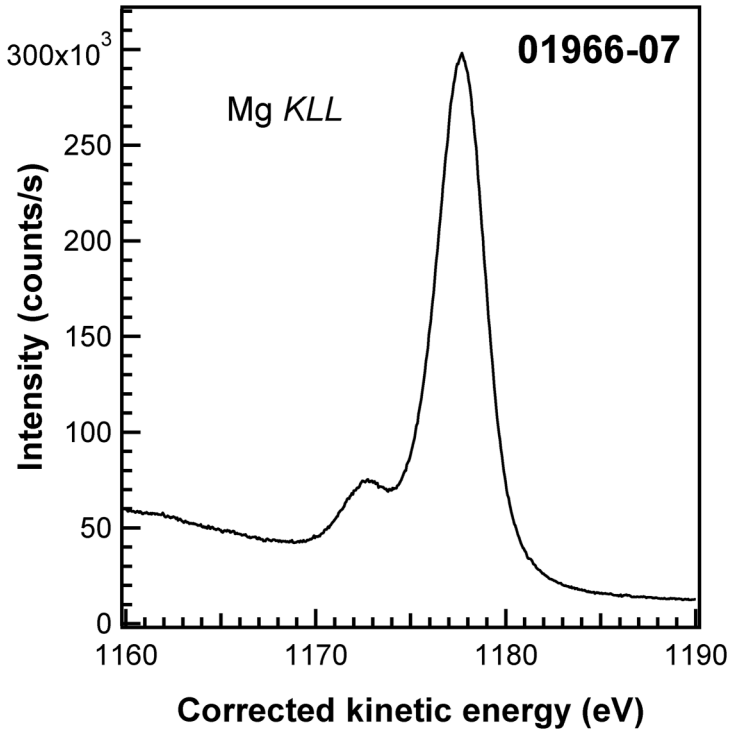

- **Accession #:** 01966-07
- **Specimen:** MgAlTi-LDH/gCN
- **Technique:** XPS
- **Spectral Region:** Mg KLL

Instrument: ThermoFisher Scientific EscalabTM QXi
Excitation Source: Al K_α monochromatic
Source Energy: 1486.6 eV
Source Strength: 200 W
Source Size: 0.50 × 0.50 mm^2
Analyzer Type: Spherical sector
Incident Angle: 58°
Emission Angle: 0°
Analyzer Pass Energy: 50 eV
Analyzer Resolution: 0.5 eV
Total Signal Accumulation Time: 152.2 s
Total Elapsed Time: 167.4 s
Number of Scans: 2
Effective Detector Width: 0.5 eV

10 October 2024 12:21:42

© Author(s) 2024

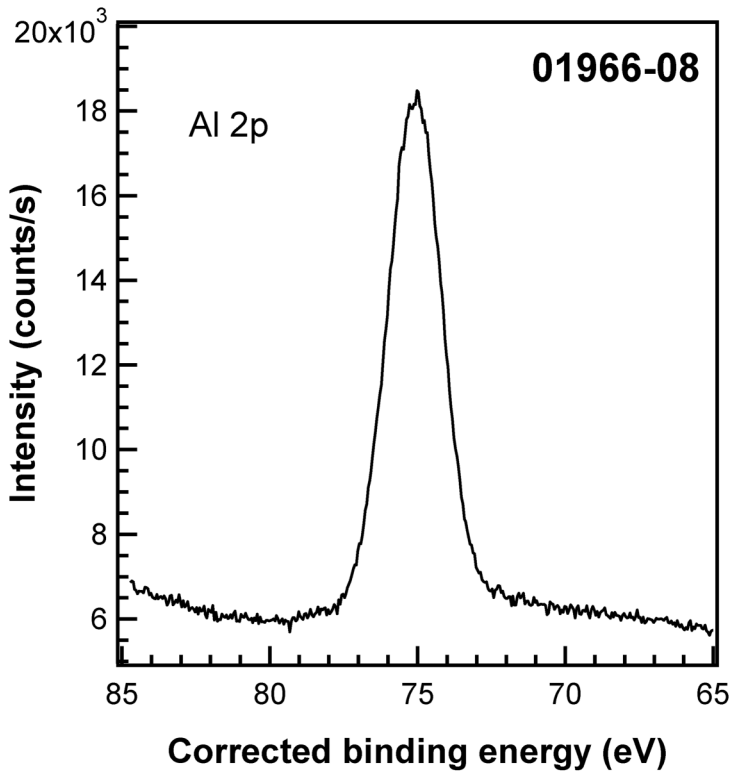

- **Accession #:** 01966-08
- **Specimen:** MgAlTi-LDH/gCN
- **Technique:** XPS
- **Spectral Region:** Al 2*p*

Instrument: ThermoFisher Scientific EscalabTM QXi
Excitation Source: Al K_α monochromatic
Source Energy: 1486.6 eV
Source Strength: 200 W
Source Size: 0.50 × 0.50 mm^2
Analyzer Type: Spherical sector
Incident Angle: 58°
Emission Angle: 0°
Analyzer Pass Energy: 50 eV
Analyzer Resolution: 0.5 eV
Total Signal Accumulation Time: 200.5 s
Total Elapsed Time: 220.6 s
Number of Scans: 5
Effective Detector Width: 0.5 eV

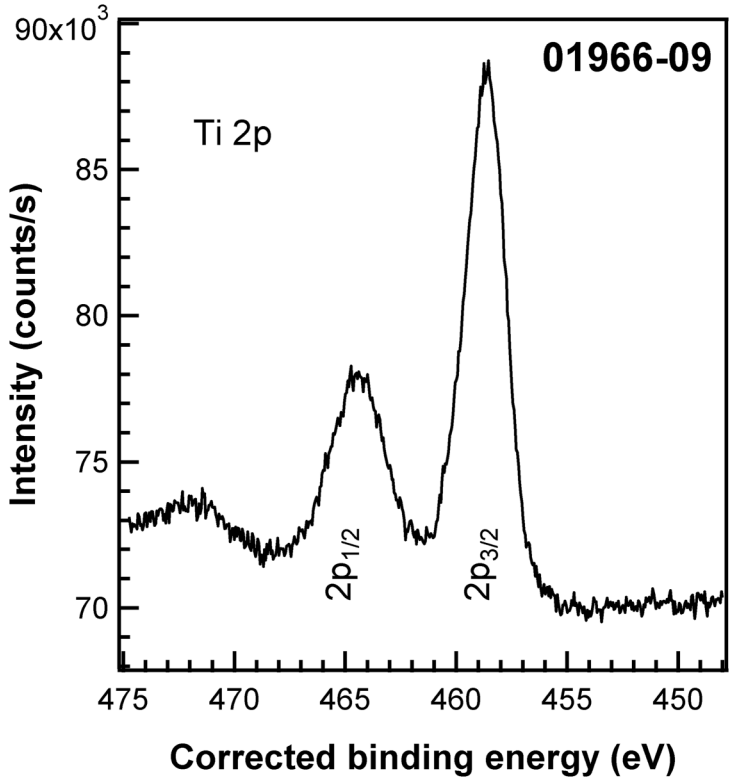

- **Accession #:** 01966-09
- **Specimen:** MgAlTi-LDH/gCN
- **Technique:** XPS
- **Spectral Region:** Ti 2*p*

Instrument: ThermoFisher Scientific EscalabTM QXi
Excitation Source: Al K_α monochromatic
Source Energy: 1486.6 eV
Source Strength: 200 W
Source Size: 0.50 × 0.50 mm^2
Analyzer Type: Spherical sector
Incident Angle: 58°
Emission Angle: 0°
Analyzer Pass Energy: 50 eV
Analyzer Resolution: 0.5 eV
Total Signal Accumulation Time: 541.0 s
Total Elapsed Time: 595.1 s
Number of Scans: 10
Effective Detector Width: 0.5 eV

10 October 2024 12:21:42

© Author(s) 2024

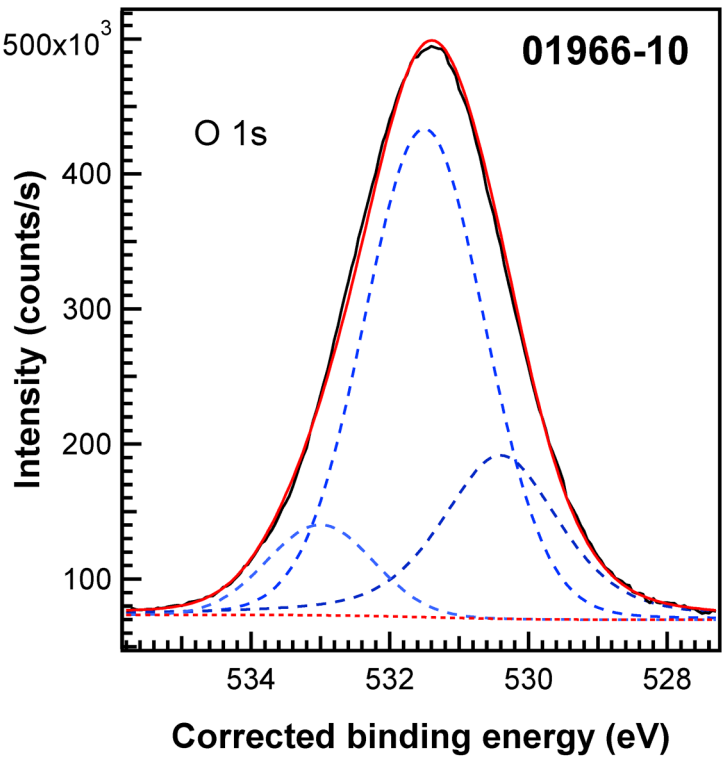

- **Accession #:** 01966-10
- **Specimen:** MgAlTi-LDH/gCN
- **Technique:** XPS
- **Spectral Region:** O 1*s*

Instrument: ThermoFisher Scientific EscalabTM QXi
Excitation Source: Al K_α monochromatic
Source Energy: 1486.6 eV
Source Strength: 200 W
Source Size: 0.50 × 0.50 mm^2
Analyzer Type: Spherical sector
Incident Angle: 58°
Emission Angle: 0°
Analyzer Pass Energy: 50 eV
Analyzer Resolution: 0.5 eV
Total Signal Accumulation Time: 80.2 s
Total Elapsed Time: 88.2 s
Number of Scans: 2
Effective Detector Width: 0.5 eV

10 October 2024 12:21:42

© Author(s) 2024